30TH INTERNATIONAL COSMIC RAY CONFERENCE

**Determination of ICME Geometry and Orientation
from Ground Based Observations of Galactic Cosmic Rays**

T. Kuwabara [1], J. W. Bieber [1], P. Evenson [1], K. Munakata [2], S. Yasue [2], C. Kato [2],
Z. Fujii [3], M. L. Duldig [4], J. E. Humble [5], M. R. Silva [6], N. B. Trivedi [6],
W. D. Gonzalez [6], A. Dal Lago [6], and N. J. Schuch [7].

[1] *Bartol Research Institute and Department of Physics and Astronomy, University of Delaware*
[2] *Physics Department, Shinshu University* [3] *STE Laboratory, Nagoya University*
[4] *Australian Antarctic Division* [5] *School of Mathematics and Physics, University of Tasmania*
[6] *National Institute for Space Research* [7] *Southern Regional Space Research Center - CRS/INPE*

takao@bartol.udel.edu

Abstract: We have developed a method for determining ICME (Interplanetary coronal mass ejection) geometry from galactic cosmic ray data recorded by the ground-based muon detector network. The cosmic ray density depression inside the ICME, which is the cause of a Forbush decrease, is represented as an expanding cylinder that is based on a theoretical model of the cosmic ray particle diffusion. ICME geometry and orientation are deduced from observed time variations of density and density gradient, and are compared with that deduced from a magnetic flux rope. From March 2001 to May 2005, 11 ICME events that produced Forbush decreases >2% were observed, and clear variations of the density gradient due to ICME passage were observed in 8 of 11 events. In 3 of these 8 events, clear signatures of magnetic flux rope structure (large, smooth rotation of magnetic field) were also seen, and the ICME geometry and orientation deduced from the two methods were very similar. This suggests that the cosmic ray-based method may provide a more robust method for deducing ICME geometry than the flux rope method for events where a large Forbush decrease is observed.

Introduction

Owing to the large detector mass required to detect high-energy cosmic rays, ground-based instruments remain the state-of-the-art method for studying these elusive particles. Muon detectors record secondary cosmic rays created by interactions of >1 GeV primary cosmic rays with Earth's atmosphere. These cosmic rays are the dominant source of ionization in Earth's atmosphere. In addition, at energies up to ∼100 GeV, primary galactic cosmic rays experience significant variation in response to passing solar wind disturbances such as interplanetary coronal mass ejections (ICMEs).

ICMEs and their accompanying shocks propagate through interplanetary space and reach Earth. Some ICMEs have a rope-like magnetic structure called a magnetic flux rope, and such structures can be a factor in producing geomagnetic storms. De-termination of ICME geometry and orientation at 1 AU is of interest for understanding the interaction of the structure with Earth's magnetosphere, and has been done by several methods. For example, fitting observations based upon a model magnetic flux rope is perhaps the most commonly employed method for determining the magnetic field inside the ICME and the ICME geometry [1].

More recently, several studies find that modeling the high energy cosmic ray density inside the ICME can also be used to determine ICME geometry and orientation [2]. Behind the shock (if present) and inside the ICME, there is a cosmic ray density-depleted region that is the cause of a Forbush decrease [3]. Within and around this depleted region, there is a "B×grad(n)" drift flow originating with the particle gyro-motion and the density (n) gradient perpendicular to the magnetic field (B). This density gradient depends on the structure

of the depleted region, and is calculated from the direction of drift flow and the interplanetary magnetic field (IMF) vector [4]. The method works by comparing the time variation of the density gradient with that expected based on a theoretical model of the cosmic ray density depleted region [5]. In this way we can determine the ICME geometry and orientation from the model calculation.

Observation of the Cosmic Ray Density and Density Gradient

Cosmic ray density, and drift flow that determine density gradient, are observed from the ground based muon detector network. Three multidirectional muon detectors at Nagoya(Japan), Hobart (Australia), and São Martinho (Brazil) that had been operated by March 2001 to May 2005 are used in this work. Network data are fitted to the function defined by using the "coupling coefficients" [6], and cosmic ray density $I(t)$ and the anisotropy vector in space $\boldsymbol{\xi}(t)$ are derived as a function of time [2]. Following *Bieber and Evenson* [4] , we calculate the fractional density gradient $\boldsymbol{g}_\perp(t)$ perpendicular to the IMF, as

$$\boldsymbol{g}_\perp(t) = R_L \frac{\nabla_\perp N}{N} = -\mathbf{b}(t) \times \boldsymbol{\xi^w}(t), \qquad (1)$$

where R_L is the particle Larmor radius, and $\mathbf{b}(t)$ is a unit vector in the direction of the IMF. In this equation, the anisotropy in the solar wind frame $\boldsymbol{\xi^w}(t)$ is derived from the $\boldsymbol{\xi}(t)$ by the subtraction of the streaming due to the Compton-Getting effect of solar wind convection and earth orbital motion.

Expanding Cylinder Model for Cosmic Ray

For modeling the cosmic ray density gradient, we used the expanding cylinder model (actually, the cylinder both convects and expands) of *Munakata et al.* [5], which is a refinement of the static convecting cylinder model of *Kuwabara et al.* [2]. According to this model, the density depression $I(x)$ as a function of x, a distance from cylinder axis normalized by cylinder radius is

$$I(x) = a_0\{1 + \frac{\Gamma}{4}x^2 + \frac{\Gamma^2}{64}x^4 + \cdots\}, \qquad (2)$$

where a_0 is density depression on the cylinder axis. Γ is described by a dimensionless parameter κ_0 that related to the degree of the cross field diffusion and a cosmic ray power spectrum $\gamma = 2.7$ as, $\Gamma = 2(2 + \gamma)/(3\kappa_0)$.

Cosmic ray density predicted at Earth are derived from this density distribution by assuming a vector $\mathbf{P}_E(t)$ that pointing the Closest Axial Point (CAP) on the cylinder axis from Earth at time t. With this vector $\mathbf{P}_E(t)$ and cylinder radius $R(t)$, normalized radial distance $x(t)$ become

$$x(t) = \frac{|\mathbf{P}_E(t)|}{R(t)}. \qquad (3)$$

Then, expected density $I^{exp}(t)$ observed at Earth at time t are deduced by the density distribution as

$$I^{exp}(t) = a_0\{1 + \frac{\Gamma}{4}x(t)^2 + \frac{\Gamma^2}{64}x(t)^4 + \cdots\}, \quad (4)$$

and also expected density gradient vector $\boldsymbol{g}_\perp^{exp}(t)$ are deduced from $I^{exp}(t)$ as

$$\boldsymbol{g}_\perp^{exp}(t) = -\frac{R_L}{R(t)} \frac{1}{I^{exp}} \frac{dI^{exp}}{dx}\mathbf{e}_\perp(t)$$

$$= -\frac{R_L}{R(t)} \frac{a_0}{I^{exp}}\{\frac{\Gamma}{2}x(t) + \cdots\}\mathbf{e}_\perp(t), \quad (5)$$

where $\mathbf{e}_\perp(t)$ is the unit vector parallel to the $\mathbf{P}_E(t)$. Normalized Larmor radius $R_L/R(t)$ is multiplied to follow an observed density gradient.

We assume that cylinder moves as average solar wind speed $\mathbf{V}_{sw}$, and that axis is parallel to the unit vector $\mathbf{e}_{ax}$ that shows cylinder orientation. Then, vector $\mathbf{P}_E(t)$ is given by

$$\mathbf{P}_E(t) = \{\mathbf{V}_{sw} - (\mathbf{e}_{ax} \cdot \mathbf{V}_{sw})\mathbf{e}_{ax}\}(t - t_c) + \mathbf{P}_c \quad (6)$$

where, t_c is the time when cylinder is closest to Earth. $\mathbf{P}_c$ is the CAP location at time t_c, i.e., $\mathbf{P}_c = \mathbf{P}_E(t_c)$, and is derived by

$$\mathbf{P}_c = d \frac{\mathbf{V}_{sw} \times \mathbf{e}_{ax}}{|\mathbf{V}_{sw} \times \mathbf{e}_{ax}|}, \qquad (7)$$

where d is the distance between Earth and CAP at time t_c. We assume that cylinder radius $R(t)$ expand with V_{exp}, become R_{in} when Earth enter cylinder at the time t_{in}, and become R_{out} when Earth exits the cylinder at the time t_{out}. Then $R(t)$

is

$$R(t) = R_{in} + V_{exp} \cdot (t - t_{in}) \tag{8}$$

$$V_{exp} = \frac{R_{out} - R_{in}}{t_{out} - t_{in}}. \tag{9}$$

In this analysis, we use average solar wind speed $\mathbf{V}_{sw}$ that is observed at satellite, and also use times that Earth encounters the cylinder boundaries, t_{in} and t_{out}, corresponding to the period of rapid variation of the density gradient. Moreover, $\mathbf{e}_{ax}$ is defined by GSE latitude θ, and longitude ϕ. Then, cosmic ray density and density gradient at Earth are functions of seven parameters, a_0, κ_0, R_L, d, θ, ϕ, and t_c.

Result and Discussion

Nearly 4 year data observed from March 2001 to May 2005 are analyzed in this work. During this period 11 ICME events that produced Forbush decreases > 2% were observed, and we used 8 events to determine ICME geometry. Three events are excluded from this analysis because there are no clear variations of the density gradient due to ICME passage. Figure 1 displays result of our model calculation for the October 29, 2003 ICME event which is the biggest event observed in analyzing period. The left side shows muon detector network observations of a Forbush decrease, cosmic ray anisotropy vector, and cosmic ray density gradient. The red lines show the model predictions, and they do a reasonable job of producing the large-scale variation of the cosmic ray density (top panel) and density gradient (lower three panels). From the best fit parameters determined in this event, ICME orientation at 1 AU is illustrated at bottom.

An ICME structure in this event is also determined from Magnetic Flux Rope calculation, and is compared with the one from cosmic ray model calculation. As shown in right side of Figure 1, signatures of the magnetic flux rope structure are seen in magnetic field and solar wind observations recorded by the ACE satellite. Red lines in the right panels show predictions of the magnetic flux rope model, and they likewise do well at reproducing the observations. Moreover, an orientation of magnetic flux rope yields very consistent results for this event.

Orientations deduced from both method for 8 events are summarized in Table 1. By compare with the magnetic field data at ACE, signatures of magnetic flux rope structure (smooth rotation of magnetic field) were seen in 5 of these 8 events. In these 5 events, the ICME geometry and orientation deduced from the two methods were very similar in 3 events, but not in the other 2 events. There is a tendency that rotations of the magnetic flux rope were relatively big in the three good agreement events. In remaining 3 events, we could not do magnetic flux rope analysis because of the small or not clear rotation of magnetic field. This suggests that the cosmic ray-based method may provide a more robust method for deducing ICME geometry than the flux rope method - the cosmic ray method provides an answer in more cases than the flux rope method, but when both methods can be applied, agreement is good.

Acknowledgements

References

[1] K. Marubashi, Physics of Interplanetary Magnetic Flux Ropes: Toward Prediction of Geomagnetic Storms, Advances in Space Research 26 (1) (2000) 55–66.

[2] T. Kuwabara, et al., Geometry of an interplanetary CME on October 29, 2003 deduced from cosmic rays, Geophysical Research Letters 31 (19) (2004) L19803.

[3] H. V. Cane, Coronal Mass Ejections and Forbush Decreases, Space Science Reviews 93 (1/2) (2000) 55–77.

[4] J. W. Bieber, P. Evenson, CME geometry in relation to cosmic ray anisotropy, Geophysical Research Letters 25 (15) (1998) 2955–2958.

[5] K. Munakata, et al., On the Cross-Field Diffusion of Galactic Cosmic Rays into an ICME, Advances in Geosciences 2 (1998) 115.

[6] K. Fujimoto, et al., Coupling Coefficients of Cosmic Ray Daily Variations for Meson Telescopes, Report of Cosmic-Ray Research Laboratory, Nagoya University 9.
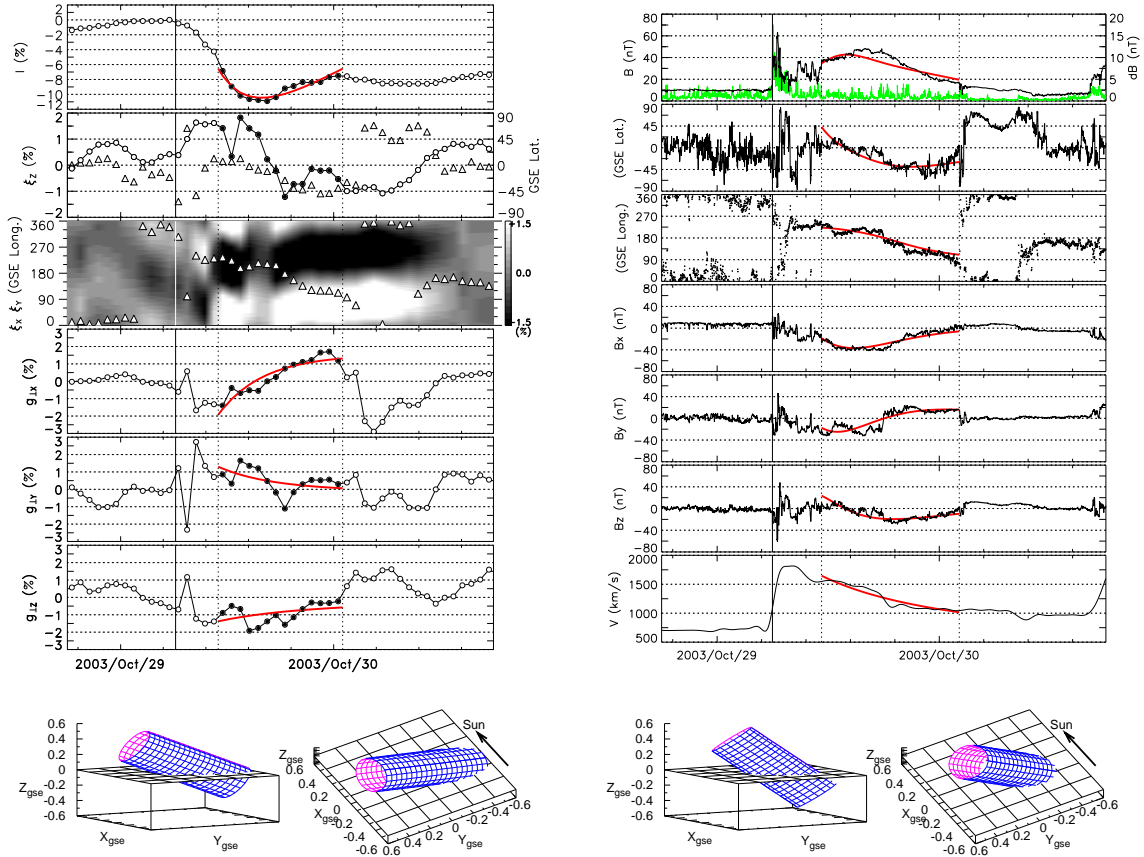
Figure 1: Observation and modeling of ICME geometry on October 29, 2003. (Left) from cosmic ray density gradients determined from prototype muon detector network and (Right) from magnetic flux rope model based upon ACE IMF measurements. Left panel: Cosmic ray density, north-south anisotropy, the component anisotropy in the ecliptic plane in a gray scale format, and the three components of the density gradient in GSE coordinates. Right panel: IMF magnitude, latitude, longitude, three Cartesian components of IMF, and the solar wind speed.

	Cosmic Ray				Magnetic Flux Rope				
Event Date	θ	ϕ	$R(t_c)$	$\mathbf{P}_c$	θ	ϕ	$R(t_c)$	$\mathbf{P}_c$	
Apr/05/2001	7	56	0.109	-0.004, 0.013,-0.067	29	277	0.175	0.000,-0.073,-0.131	
Apr/11/2001	66	12	0.060	0.000,-0.002,-0.000					
Apr/28/2001	26	283	0.097	0.001,-0.009,-0.018					
Nov/06/2001	38	273	0.074	0.000,-0.023,-0.030					
Oct/29/2003	35	78	0.215	0.000,-0.066, 0.091	46	56	0.222	0.000,-0.080, 0.064	◯
Jul/27/2004	5	303	0.096	0.000,-0.004,-0.032	16	296	0.136	0.000,-0.004,-0.012	◯
Nov/09/2004	44	187	0.065	0.001,-0.038,-0.004	36	195	0.060	0.000,-0.036,-0.013	◯
Jan/22/2005	7	337	0.049	0.000,-0.003,-0.007	51	212	0.237	0.000,-0.170,-0.074	

Table 1: Geometries and orientations of ICME at 8 events. Event date, inclination (latitude θ and longitude ϕ in GSE) and radius $R(t_c)$ of the cylinder, and impact parameter P_c deduced from cosmic ray-based method and flux rope method. Three events that very similar ICME geometry and orientation are deduced from the two methods, are marked in the right column.